Hindawi Publishing Corporation
Journal of Industrial Mathematics
Volume 2014, Article ID 460857, 16 pages
http://dx.doi.org/10.1155/2014/460857

Research Article

Mathematical Model of a Flash Drying Process

Erik W. Aslaksen

Gumbooya Pty Ltd. 3 Gumbooya Street, Allambie Heights, NSW 2100, Australia

Correspondence should be addressed to Erik W. Aslaksen; erik@gumbooya.com

Received 16 September 2013; Revised 13 December 2013; Accepted 23 December 2013; Published 24 February 2014

Academic Editor: Santiago Laín

The paper presents a basic model of the flash drying process, as it is applied in a number of industrial applications, and illustrates this by means of a particular application: the drying of subbituminous coal. Besides its economic importance, that application is representative of those where the product is combustible, so that the drying needs to be conducted in an inert atmosphere, which is achieved by recycling some of the drying gas. A novel feature of the model is that it takes explicit account of the transport of heat and moisture within the coal particles. The model provides the basis for the development of a tool to support the design of a flash drying plant.

1. Introduction

1.1. Background. Flash drying is the process of drying particulate matter by exposing it briefly (typically a few seconds) to a high temperature gas stream, resulting in a rapid rate of evaporation without excessive heating of the product. The process is used in various industries, such as the food and wood processing industries, and a considerable literature exists on the design and modelling of the process [1]. However, a literature survey carried out in 2009, when this work was undertaken, did not find any comprehensive models of the process suitable as a basis for plant design [2]. In particular, while individual research papers treat both particle size and shape (see Section 3.6) and particle-gas heat transfer (see Section 4.1), these results do not appear to have been integrated into a design model. The present monograph focuses on the application of the process to the drying of coal, but the basics of the process remain the same for its application in other industries, and the model developed here has a correspondingly general validity.

There are at least three reasons for the focus on coal and, in particular, on the drying of subbituminous coal as an example for the purpose of developing a detailed model suitable for numerical calculations. The first is that pulverised coal is a difficult material to handle, and of the many dryers that have been constructed over the last several decades, only very few remain in operation, the rest having succumbed to fire and/or explosions or simply been abandoned due to related operational problems. Similar problems arise in some other industries, for example, in the drying of wood fibres.

The second reason is that the last 20 years have seen renewed interest in drying subbituminous coal, with large deposits being found in the US Midwest, in China, Mongolia, and on Kalimantan. Subbituminous coal lies between lignite and bituminous coal in this development sequence and is characterised by a water content in the range 10–40%, carbon content in the range 35–45%, and calorific values in the range 10–20 MJ/kg. Compared with bituminous coal it has the advantage of low sulphur content (typ. 0.25%) and low ash content (typ. 5%), but its disadvantage is the high water content and thereby lower calorific value, which is detrimental to two important utilisations of the coal. Firstly, when the coal is burned in a boiler, the flame temperature is lower due to the water vapour, and so the boiler surfaces need to be larger to transfer the required amount of heat. Conversely, if subbituminous coal is used in a boiler designed for bituminous coal, the power rating is reduced. So, as a consequence, there would be considerable value in converting subbituminous coal to bituminous coal by removing some or all of the water content.

Secondly, the current concerns regarding CO_2 emissions are driving efforts to increase the efficiency of coal as a fuel for electricity generation and to capture and store the CO_2. Prominent among the former is the gasification of coal in

order to use it as a fuel in combined cycle plants, and in order to gasify lower rank coals, such as subbituminous coal and brown coal (or lignite), they need to be dried as a first stage of the process.

1.2. Structure of the Paper. Following the listing of some material parameter values in the next subsection, the mathematical model is developed in the following four sections. Section 2 defines the process and its parameters and looks at its basic thermodynamic properties and operating characteristics. Section 3 discusses the mechanical interaction between the coal particles and the drying gas and the influence of the size distribution of the coal particles. Section 4 develops a model of the thermal interaction between the coal particles and the drying gas, including a number of detailed aspects of this interaction. Section 5 is concerned with several issues that need to be considered when creating a computer application for the numerical evaluation of the model.

1.3. Parameter Values. Throughout this monograph we shall be assuming the coal to be a typical subbituminous coal with the following characteristics.

Proximate Analysis:

total moisture: 32.3% (range 31–35%)

ash: 3.9%

volatiles: 33.5%

fixed carbon: 30.3%.

Ultimate Analysis (Coal Has Been Dried, but the Ash Is Included):

carbon: 68.3%

hydrogen: 5.26%

nitrogen: 0.93%

oxygen: 19.7%

sulfur: 0.15%

total: 94.34%

ash: 5.66%.

The specific heat capacity of this coal is 1.2 J/g/°C.

We shall also be using the following constants and values for material properties:

(a) standard atmosphere:

(i) temperature: 0°C
(ii) pressure: 101.3 kPa
(iii) density: 1.293 kg/m^3

(b) composition of dry air (by mass): 75.52% N_2, 23.13% O_2, 1.29% Ar, 0.06% various

(c) mean molecular weight of air: 28.97

(d) vapour pressure of water as shown in Table 1

(e) the heat of vaporisation of water: 2.255 kJ/g.

Unless otherwise stated, all equations and expressions assume that the variables are measured in SI units.

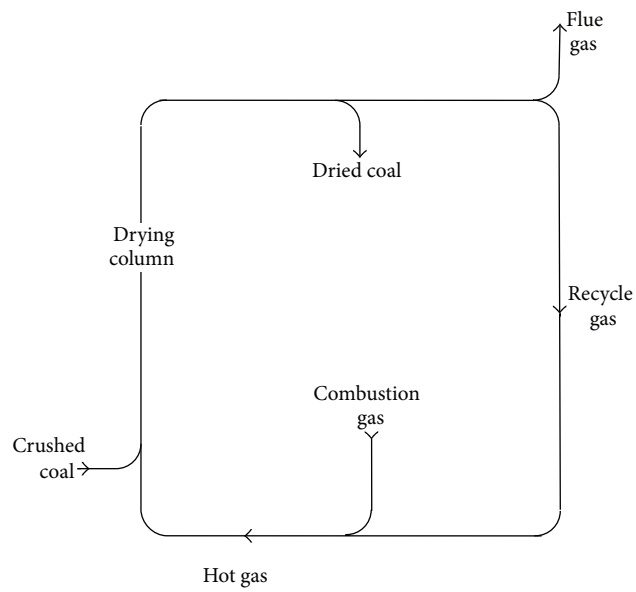

Figure 1: The drying circuit, illustrating how a fraction of the gas exiting from the drying process is recycled and combined with the combustion gas in order for the oxygen content of the hot gas that enters the drying column to be below the explosion limit, that is, inert.

2. Basic Properties and Relations

2.1. Drying Circuit and Associated Parameters. As was indicated in the Introduction, an important aspect of this particular model is that the material to be dried, that is, coal dust, is highly combustible. This then requires the drying to take place in an inert atmosphere (see Section 3.7), and the inert atmosphere is created by recycling some of the gas exiting the drying process and mixing it with the combustion gas to make up the hot gas injected into the drying process.

The drying circuit consists of a drying column, in which *crushed coal* is injected into an upward flow of *hot gas* in the lower part of the column. At the top of the column, a mixture of gas and *dried coal* exits the column and the coal is separated from the gas. A proportion of the gas is exhausted to atmosphere, and the rest, the *recycle gas*, is mixed with the *combustion gas* to produce the hot gas. This is illustrated schematically in Figure 1.

2.1.1. In All That Follows, the Rate of Dried Coal Produced Will Be Normalised to 1 kg/s. The *parameters* of this process are as follows:

moisture content of the crushed coal: x,

moisture content of the dried coal: y,

ambient temperature: T_a (°C),

temperature of the hot gas: T_x (°C),

fraction of exit gas recycled: η,

flow of combustion gas: g (kg/s),

Table 1

°C	100	101	102	103	104	105	106	107	108	109	110
kPa	101.3	105.0	108.7	112.6	116.6	120.8	125.0	129.3	133.9	138.5	143.2

coal analysis (dry basis):

Carbon: c_1,
Hydrogen: c_2,
Oxygen: c_3,
Ash: c_4,

fraction of water in gas: ω,

fraction of nitrogen in dry gas: λ.

The *assumptions* made about this process, which are justified by practical plant design considerations, are as follows.

(i) The fuel used to generate the combustion gas is dried coal.

(ii) The burner operates with 20% excess air.

(iii) The nitrogen and sulphur content of the coal is negligible (as far as the drying process is concerned).

(iv) The gas temperature at the drying column exit is 140°C.

(v) The average temperature of the dried coal is 110°C.

(vi) Heat losses are 5% and occur mainly in the furnace and hot gas part of the circuit.

(vii) The separation of dried coal from the gas is 100% efficient.

(viii) The distribution of crushed coal and gas is uniform over the cross-section of the drying column at every level.

(ix) Crushed coal and combustion air are both at ambient temperature.

Some of these assumptions will be reexamined in later chapters, and it is not difficult to see what the consequences of a change to any one of these assumptions would be. The purpose of making these assumptions is to simplify the presentation of the basic relations and to allow numerical analysis to be carried out with a reasonable amount of effort.

2.2. Basic Relationships. The amount of crushed coal entering the drying column is given by the expression

$$\frac{1-y}{1-x}. \tag{1}$$

Consequently, the amount of water to be extracted from the coal, evaporated and exhausted to atmosphere per second, is given by the expression

$$\frac{x-y}{1-x}. \tag{2}$$

The total exhaust flow is this amount plus the combustion gas flow, g, and so it follows that the recycle gas flow equals

$$\left(g+\frac{x-y}{1-x}\right)\frac{\eta}{1-\eta}, \tag{3}$$

and the hot gas flow is just this plus the combustion gas or

$$\frac{g+\eta\left((x-y)/(1-x)\right)}{1-\eta}. \tag{4}$$

2.3. Energy Balance. The power required to produce 1 kg/s of dried coal has the following components:

heating the coal from T_a to 11°C: $(1-y)\cdot 1.2\cdot(110-T_a)$(kW) ,

heating the water from T_a to 100°C: $x(1-y)/(1-x)\cdot 4.184\cdot(100-T_a)$ (kW),

vaporising part of the water: $(x-y)/(1-x)\cdot 2255$ (kW),

heating the vapour from 100°C to 140°C: $(x-y)/(1-x)\cdot 2.05\cdot 40$ (kW),

where the specific heat of coal has been taken as 1.2 J/g/°C, that of superheated steam, averaged over the temperature range of 100°C to 140°C, as 2.05 J/g/°C, and the heat of vaporisation of water as 2.255 kJ/g. Adding these components together, the power required, E, in kW, is

$$E = 2337\frac{x-y}{1-x}+(1-y) \times\left[\frac{x}{1-x}\left(418.4-0.01T_a\right)+132-1.2T_a\right]. \tag{5}$$

This energy has to be delivered by the hot gas as its temperature declines from T_x to 140°C, that is, the difference in enthalpy, per kg, of the gas at T_x and 140°C, multiplied by the hot gas flow. The specific enthalpy difference is given by the expression

$$\int_{140}^{T_x} c_p(T)\,dT, \tag{6}$$

and so it is necessary to determine $c_p(T)$, the heat capacity at constant pressure as a function of temperature.

Unless stated otherwise, the hot gas shall be defined as having the following composition (fractions by weight):

nitrogen: $\lambda(1-\omega_h)$,

carbon dioxide: $(1-\lambda)(1-\omega_h)$,

water: ω_h,

where ω_h is the water content in the hot gas, and the small amount of oxygen present in the hot gas is counted in with the nitrogen for the purpose of determining the specific heat. The specific heat of the hot gas is the weighted sum of the specific heats of these three components. The individual specific heats are determined in Section 2.5, and the value of λ will be determined in the next subsection; it remains to determine the value of ω_h.

Let the water content of the combustion gas be denoted by ω_c (see next subsection); then the amount of water in the hot gas is given by the expression

$$g\omega_c + \frac{\eta(x-y)}{(1-\eta)(1-x)}, \tag{7}$$

$$\omega_h = \frac{g\omega_c(1-x)(1-\eta)+\eta(x-y)}{g(1-x)+\eta(x-y)}. \tag{8}$$

2.4. The Combustion Gas. The quantity of combustion gas required to produce the energy 1.05E (taking into account the 5% heat loss) is determined by the calorific value of the dried coal, which is again determined by the composition of the coal. Using Dulong's formula, the heating value, HV, is given by

$$\mathrm{HV} = 33950 \cdot c_1 + 144200\left(c_2 - \frac{c_3}{8}\right)\ (\mathrm{kJ/kg}), \tag{9}$$

where c_i are the component fractions by weight, as defined in Section 2.1.1.

For coal with a moisture content y, there are then two heating values: a gross heating value, HHV, which assumes that all combustion components are brought back to ambient temperature, and the net heating value, LHV, which assumes that the water vapour in the combustion gas is not condensed and which is the one appropriate for the drying process. Consider

$$\mathrm{HHV} = \mathrm{HV}(1-y) \tag{10}$$

$$\mathrm{LHV} = \mathrm{HHV} - 2400(y + 9\cdot c_2)\quad (\mathrm{kJ/kg}). \tag{11}$$

The next step is to determine the amount of air required to combust 1 kg/s of dry coal. The mass flow of dry air required for the stoichiometric combustion of 1 kg/s of coal is given by

$$W_a' = 4.35\cdot(2.67\cdot c_1 + 8\cdot c_2 - c_3)\quad (\mathrm{kg/s}). \tag{12}$$

The combustion air will contain some moisture. If the relative humidity is denoted by ε, then a good approximation for the water content, r, in g/m^3 at 101.3 kPa and ambient temperature T_a, is given by the expression

$$r = \varepsilon\cdot\left(0.021\cdot T_a^2 + 0.21\cdot T_a + 4.9\right), \tag{13}$$

obtained by fitting a second-order function to data points provided in the *Handbook of Chemistry and Physics* [4]. The stoichiometric quantity of moist combustion air, W_a, can then be closely approximated by

$$W_a = W_a'\left(1 + \frac{r}{1200}\right). \tag{14}$$

Table 2: Mass of combustion gas components, resulting from the combustion of 1 kg of dry coal with components c_i and using an excess air fraction κ.

Component	Mass (kg)
CO_2	$c_1\cdot 3.67$
H_2O	$c_2\cdot 9 + 0.00083(1+\kappa)W_a\cdot r$
N_2	$W_a(1+\kappa)\cdot(0.77 - 0.00083\cdot r)$
O_2	$\sigma\cdot W_a\cdot 0.23$
Ash	c_4
Total	$(1+\kappa)\cdot W_a+1$

This value needs to be multiplied by a factor $(1+\kappa)$, where κ is the *excess air fraction*, as there needs to be some excess oxygen in the combustion gas in order to ensure complete combustion and a correspondingly low level of CO. In accordance with assumption (ii) of Section 2.1, $\kappa = 0.2$.

The composition of the combustion gas can now be calculated. For 1 kg of dry coal combusted, the mass of the various components is shown in Table 2.

If the dried coal has a moisture content of y, then the values in Table 2 need to be multiplied by $(1-y)$ in order to apply to the combustion of 1 kg of dried coal (rather than dry coal).

The third step is to apply a small correction. As the heating values are defined assuming that the combustion gases are returned to ambient temperature, we would have to correct this LHV by taking into account the energy lost through the combustion gas exhausted to atmosphere at 140°C. Instead, we add that energy lost, per second and kg of dried coal, to E. If we take the specific heat capacity of the combustion gas to be constant and equal to 1 J/g/°C, this correction, Δ_e, equals

$$\Delta_e = g\cdot(140 - T_a)\quad (\mathrm{kJ/kg\cdot s}). \tag{15}$$

The amount of fuel required to produce 1 kg/s of dried coal is therefore given by the expression

$$\frac{1.05\cdot E + \Delta_e}{\mathrm{LHV}}\quad (\mathrm{p.u.}), \tag{16}$$

and combining this with the earlier equations (2.5/9/11/12/13/14/15) determines the value of g for any given coal,

$$g = \frac{1.05E\left(W_a(1+\kappa)(1-y)+1\right)}{\mathrm{LHV} - (140 - T_a)\left(W_a(1+\kappa)(1-y)+1\right)}. \tag{17}$$

The amount of nitrogen (plus oxygen and ash) produced by combusting 1 kg of dried (not dry) coal is determined by the corresponding expressions in Table 2, or $W_a(0.97 - -0.000996\cdot q + 0.046 + c_4)(1-y)$, and the expression for λ is

$$\begin{aligned}\lambda = {} & \left(W_a\left(1.016 - 0.000996\cdot r + c_4\right)(1-y)\right.\\ & \left.\times\left(1.05E + g(140 - T_x)\right)\right)\\ & \times(g\cdot\mathrm{LHV})^{-1}.\end{aligned} \tag{18}$$

The water content of the combustion gas, ω_c, is also given by the corresponding expression in Table 2, plus the water content in the dried coal,

$$\omega_c = \Big(\big(y + (9c_2 + 0.00083\,(1+\kappa)\,W_a \cdot r)\,(1-y)\big) \times \big(1.05E + g\,(140 - T_x)\big) \Big) \times (g \cdot \mathrm{LHV})^{-1}. \tag{19}$$

Regarding the composition of the hot gas, the fraction of water, ω_h, is now a function of η only, in accordance with (8). However, to determine the value of η as a function of the hot gas temperature, T_x, we need to know the enthalpy of the hot gas.

2.5. Heat Capacities and Enthalpy. As discussed in Section 2.3, we require the specific heat capacities, as functions of temperature, for the three components of the hot gas: nitrogen, carbon dioxide, and superheated steam. Using the values given in *Gas Tables*, by Keenan, Chao, and Kaye [20], we find the following very good approximations for the temperature range of interest:

$$\begin{aligned} &\text{nitrogen: } c_p{}^n(T) = 1.00951 + 0.000213 \cdot T \quad (\mathrm{J/g/^\circ C}) \\ &\text{carbon dioxide: } c_p{}^c(T) = 0.9293 + 0.000413 \cdot T \quad (\mathrm{J/g/^\circ C}) \\ &\text{steam: } c_p{}^s(T) = 1.664 + 0.0008 \cdot T + 32.4/T \quad (\mathrm{J/g/^\circ C}). \end{aligned} \tag{20}$$

In addition, there is the ash component. The specific heat capacity of fly ash is, according to published values (e.g., http://www.scotash.com/), about 0.75 J/g/°C and is practically constant with temperature in the range of interest here. However, as the ash content is less than 10%, the fuel coal makes up less than 10% of the combustion gas, and the combustion gas makes up less than half of the hot gas; it is a very good approximation to just lump the ash in with the dry gas (as was already done in (10)).

The specific enthalpy of the dry gas component is $\lambda c_p{}^n + (1-\lambda) c_p{}^c$, and the specific enthalpy difference, as defined by (6), of this component is given by the expression

$$h_g = (0.9293 + 0.08021 \cdot \lambda)\,(T_x - 140) + (0.0002065 - 0.0001 \cdot \lambda)\,(T_x - 140)^2. \tag{21}$$

The specific enthalpy difference of the superheated steam is given by the expression

$$h_s = 1.664\,(T_x - 140) + 0.0004(T_x - 140)^2 + 32.4 \cdot \ln(T_x - 140). \tag{22}$$

2.6. Operating Point. The drying energy, which is provided by the hot gas, depends on the temperature of the gas and the rate of flow of gas. That is, the same amount of energy can be provided by a lower temperature and a higher flow rate or a higher temperature and a lower flow rate. For given values of x and y, the choice of the hot gas temperature, T_x, determines the *operating point* of the dryer.

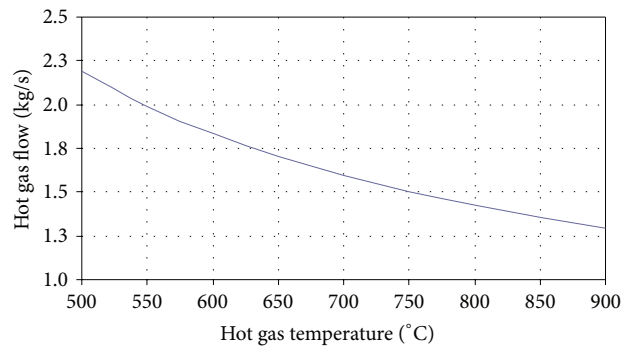

Figure 2: Rate of flow, F, in kg/s (vertical axis), versus temperature, T_x, in °C (horizontal axis), of hot gas for the production of 1 kg/s of dried coal, reducing the moisture from 33% to 6%.

The hot gas flow rate is given by (4); this multiplied by the specific enthalpy difference must equal the required drying power, E, or

$$\left(g + \eta \frac{x-y}{1-x}\right)\left[(1-\omega_h)\,h_g + \omega_h h_s\right] = (1-\eta)\,E, \tag{23}$$

and inserting (8) for ω_h, we find that this relationship becomes a quadratic equation determining the remaining variable, the recycle ratio, η:

$$a\eta^2 + b\eta + c = 0, \tag{24}$$

where the coefficients are given by

$$\begin{aligned} a &= g\omega_c\,(1-x)\,(x-y)\,(h_s + h_g) + (2h_g - h_h)\,(x-y)^2; \\ b &= g^2\omega_c(1-x)^2\,(h_g - h_s) + g\,(1-x)\,(x-y)\,\big(2h_s + h_g\,(3-\omega_c)\big) + E\,(1-x); \\ c &= g^2\,\big(\omega_c(1-x)^2\,(h_s - h_g) + h_g(1-x)^2\big) - E\,(1-x). \end{aligned} \tag{25}$$

Once the recycle ratio, η, has been determined, the water content of the hot gas, ω_h, is given by (8), and the relationship between temperature, T_x, and the rate of flow, F, of the hot gas is fixed; an example is shown in Figure 2.

3. Gas-Particle Dynamics

3.1. Particle Size Distribution

3.1.1. Introduction. Material produced by crushing or milling is commonly characterised by a particle size distribution determined by *sieving*, that is, by passing a sample of the material through a succession of sieves, $i = 1, \ldots, n$, with decreasing mesh openings, a_i, with $a_i > a_{i+1}$. For simplicity,

Table 3: Isometric particle characteristics.

Isometric Particle	Max dimension	Volume	Surface	Sphericity
Cube, with edges s	$s = a$	a^3	$6\,a^2$	0.806
Sphere, with diameter s	$s = a$	$0.5236\,a^3$	$3.1416\,a^2$	1.0
Tetrahedron, with edges s	$s = a/\cos(15^\circ)$	$0.13054\,a^3$	$1.8564\,a^2$	0.67

the mesh openings are assumed to be square. Let the fraction of the sample contained in sieve i be denoted by q_i; in the limit of $a_i - a_{i-1} \rightarrow 0$, we can introduce the function $q(a)$, with $q(a)da$ being the fraction of material (by weight) between a and $a + da$.

The particles making up the sample in one sieve will show a range of shapes and volumes, and, depending on the application, the sieving results have to be interpreted and applied appropriately. In a number of applications it is common to treat the particles as if they were spherical, with a diameter s determined by the sieve opening, that is, $s = a$, and then correct for the fact that the particles are not really spherical by introducing a *sphericity factor*, ψ, defined as the ratio of the surface area of a sphere to that of the particle when both have the same volume. The purpose of Section 3.1 is to examine the effect of this approach in the case of flash drying of particulate matter, which involves both the dynamics of the particles in a gas stream and their thermal interaction with the gas.

3.1.2. Isometric Particles. Our investigation focuses on the case where the particles are assumed to be isometric (i.e., have similar dimensions in three orthogonal directions). The choice is based both on previous published work in pneumatic conveying [5–7] and on a visual examination of a sample of subbituminous coal that has passed through a cage mill that was adjusted to give nominally a −3 mm product, and it is acknowledged that this limits the generality of this investigation, as the particle shape depends on both the material and the manner of its processing, with milling usually giving particle shapes closer to spherical than crushing [8].

Consider the largest (in dimension) isometric particles that will pass through a sieve with opening a as shown in Table 3.

So, if we again consider two sieves, the top one with opening $a + da$ and the bottom one with opening a, the particles on the bottom sieve will have volumes ranging from 0.2493 to 1.91 times that of a sphere with volume $\pi a^3/6$. Or, by expressing the volumes in terms of the diameter of spheres with the same volumes, the diameters range from $0.6294a$ to $1.241a$.

The distribution of particle sizes on the sieve with opening a is generally not known, but in the absence of any further information, the simplest assumption by far is that the probability density function of particle volumes, $p_a(V)$, as measured by the diameter of the sphere of equivalent volume,

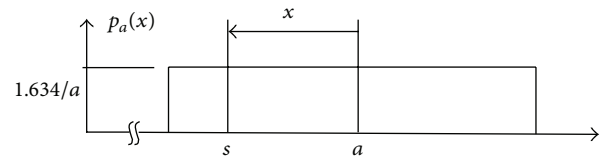

Figure 3: The function $p_a(x)$, representing the contribution of the fraction of the sample on the sieve with opening a to the density of particles with a volume of $\pi s^3/6$.

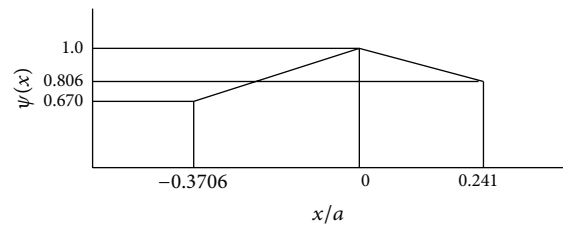

Figure 4: The assumed linear dependence of the sphericity factor, ψ, on the deviation of diameters, x, from the sieve opening, a.

is uniform over the range 0.2493 to 1.91 times that of a sphere with volume $V_0 = \pi a^3/6$. That is, the fraction of the sample with diameters between s and $s+ds$ on the sieve with opening a is given by $p_a(V(s)) \cdot ds = C_a \cdot ds$, and as

$$\int_{0.6294a}^{1.241a} C_a \cdot ds = 1, \tag{26}$$

we find that $C_a = 1.634/a$.

Consider now the situation illustrated in Figure 3, in which particles contained in the sieve with opening $a = s - x$ contribute to the density of particles with volume $\pi a^3/6$, which will be denoted by $f(s)$.

The probability density function $f(s)$ is then given by the expression

$$f(s) = 1.634 \int_{-0.59s}^{0.194s} \frac{q(s-x)}{s-x} dx, \tag{27}$$

and $f(s)ds$ is the fraction of particles (by weight) with volumes between $\pi s^3/6$ and $\pi(s+ds)^3/6$. The boundaries of $p_{s-x}(x)$ are given by $s = 0.6294\,(s-x)$ and $s = 1.241\,(s-x)$, or $-0.59s$ and $0.194s$.

The distribution $f(s)$ is of interest in many applications, in particular, because if ρ is the density of the particle substance (e.g., 1300 kg/m^3 for coal), then the specific number of particles (i.e., per unit mass) with diameter between s and $s + ds$, $n(s)ds$, is given by

$$n(s)\,ds = 1.91 \frac{f(s)}{\rho \cdot s^3} ds. \tag{28}$$

The value of the sphericity is indicated in Table 3, and if we assume a linear relationship between sphericity and the variable x, as shown in Figure 4, we find that the average sphericity, ψ, has the value 0.818.

The average sphericity of the particles is a somewhat contentious issue, and in light of the great differences in

Table 4: Sieving results on a sample of sub-bituminous coal milled to −3 mm, together with the fractions calculated by fitting a Weibull distribution with $\lambda = 1.065$ and $k = 1.115$.

Sieve number	1	2	3	4	5	6	7	8
Mesh opening (mm)	2.000	1.000	0.500	0.250	0.125	0.063	0.031	0.016
Fraction retained	0.136	0.268	0.231	0.124	0.103	0.079	0.037	0.022
Calculated fractions	0.155	0.255	0.243	0.163	0.091	0.047	0.023	0.011

sphericity between particle shapes, one might question if using an average is appropriate at all. That will depend on the application (e.g., abrasion, conveying, drying, combustion, etc.), but if an average value is used, how should it be determined? The shape distribution investigated above gives a value of 0.825 for isometric particles. However, the values reported in the literature are 0.78 [9] and 0.73 [10], and in [11] it is suggested that if no more accurate information is available, one should use $\psi = 0.7$. The difference between the two values, 0.825 and 0.7, is probably to be found in irregularities in real particle surfaces as compared with the smooth surfaces of the geometric shapes.

3.1.3. The Probability Density Function $q(a)$. In order to determine the pdf $f(s)$ through integration, as indicated by (27), we require an analytic expression for the pdf $q(a)$, and it is common practice to characterise particulate matter by approximating the result of a sieving analysis by the two-parameter Weibull pdf (also called a Rosin-Rammler pdf),

$$q(a;k,\lambda) = \frac{\lambda}{k}\left(\frac{a}{k}\right)^{\lambda-1} e^{-(a/k)^{\lambda}}, \tag{29}$$

where λ is the shape factor and k is the scale factor. The fraction retained on the ith sieve is given by

$$Q_i = e^{-(a_i/k)^{\lambda}} - e^{1(a_{i-1}/k)^{\lambda}}; \tag{30}$$

fitting these values of Q_i to the measured values then determines λ and k.

To see what this means in practice, consider the following results, obtained on subbituminous coal milled to −3 mm size, as shown in Table 4.

The rms error of the fit shown in Table 4 is 2.1%, but it is obvious that individual values differ considerably more, as evidenced, for example, by the values for sieve number 8. A pdf that gives a better fit is the following four-parameter function:

$$q(a;c) = \frac{2}{c_1c_2 + c_3c_4}\left[c_1 e^{-(a/c_2)}\left(1 - e^{-(a/c_2)}\right) + c_3 e^{-(a/c_4)}\left(1 - e^{-(a/c_4)}\right)\right], \tag{31}$$

and a comparison of the two functions with the sieving result is shown in Figure 5, where the parameter values are $c_1 = 0.675$, $c_2 = 0.829$, $c_3 = 1.758$, and $c_4 = 0.083$.

3.1.4. The Diameter pdf. Returning to our original quest, that of determining the function $f(s)$ defined in (27), we can now use the analytical expressions for $q(a)$. Using the Weibull pdf

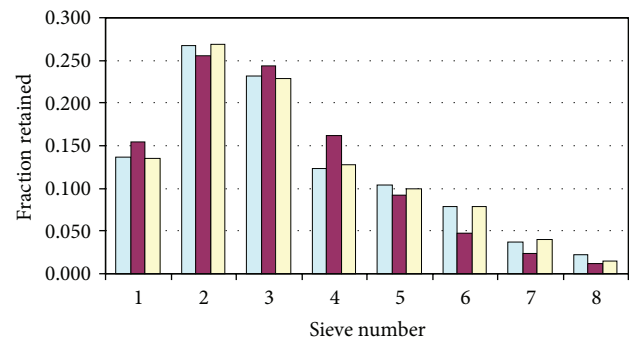

Figure 5: Comparison of the Weibull approximation (dark central bars) and the four-parameter function (bars on the right) with the measured values (bars on the left), showing that the four-parameter function provides a significantly more accurate representation of the measured values, as compared with the Weibull distribution.

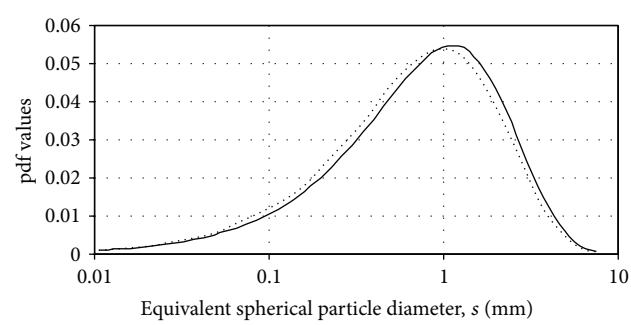

Figure 6: The full curve is the best fit of a Weibull pdf to the experimental sieving results; the dotted curve is the resulting pdf of spherical diameters.

with the values of λ and k given in the caption of Table 4, numerical integration gives the result shown in Figure 6.

The result is, as one would expect, a shift of the pdf towards smaller diameters, and performing the same calculation using the four-parameter function gives the result shown in Figure 7.

In these two figures the shift looks almost insignificant, but if we form the ratio of the shifted values to the original, for each value of s, as shown in Figure 8, we see that the correction is in the range ±15%. Expressed in terms of the average diameter, there is a shift from 0.316 mm to 0.279 mm, or 11.7%, in the case of the Weibull pdf, and from 0.273 mm to 0.242 mm, or 11.4%, in the case of the four-parameter function.

We shall return to this issue of particle shape and size distributions and their influence (if any) on the drying

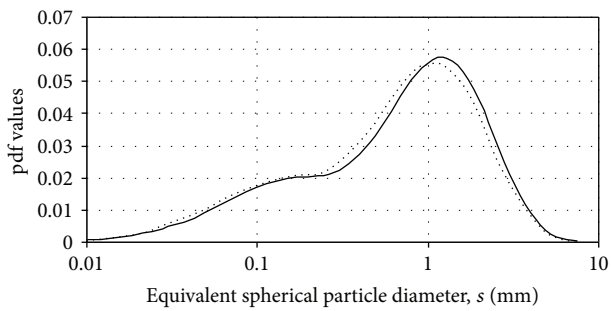

Figure 7: The full curve is the best fit of a four-parameter pdf to the experimental sieving results; the dotted curve is the resulting pdf of spherical diameters.

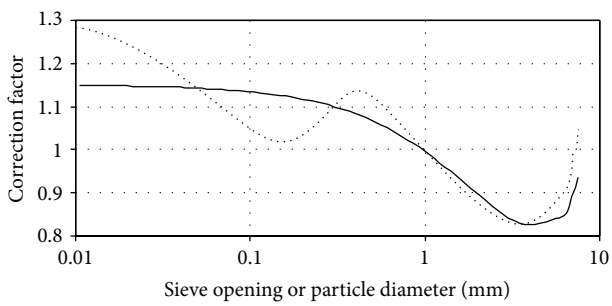

Figure 8: The correction factor that must be applied to the sieving results in order to obtain the distribution of the equivalent spherical particle diameter, s, assuming a uniform distribution of isometric particle shapes. The full curve applies to a Weibull distribution of particle sizes and the dotted curve to a four-parameter distribution.

process as the development of our understanding of the process progresses, first in Section 3.6 and then in Section 5.

3.2. The Drag Force. The force exerted by a gas stream with velocity v_r relative to the particle and density σ on a particle with cross-section A is given by the expression

$$F_d = C_d A \frac{\sigma \cdot {v_r}^2}{2}, \tag{32}$$

where C_d, the *drag coefficient*, is a factor that depends on the shape and diameter of the particle, as well as on v_r. Assuming, for the moment, a spherical shape, the dependence of C_d on diameter and velocity is usually expressed in terms of the Reynolds number, Re,

$$\mathrm{Re} = \frac{s v_r}{\nu}, \tag{33}$$

where s is the particle diameter and ν is the kinematic viscosity, μ/σ. A commonly used expression for the dependence of C_d on Re in the range of Re of interest (1 to 1000) is the following [12]:

$$C_d = 0.4 + \frac{26}{(\mathrm{Re})^{0.8}}. \tag{34}$$

We shall return to the issue of nonsphericity in Section 3.4, but to determine F_v as a function of gas velocity we first need the gas density and viscosity.

Table 5: Densities of drying gas components.

Component	Density at 100°C and 101 kPa (kg/m^3)
CO_2	1.447
N_2	0.915
H_2O	0.596

3.3. Drying Gas Characteristics. The viscosity of the three components of the gas in the drying column (nitrogen, carbon dioxide, and steam) can be found in Appendix A of [3], and by fitting linear relations to these values in the range of temperature of interest, 140–900°C, we find the following dependence on temperature (*note that, for brevity, the values of μ have been multiplied by 10^7*):

$$\begin{aligned} &\text{nitrogen:} \quad \mu = 64.85 + 0.365 \cdot T; \\ &\text{carbon dioxide:} \quad \mu = 36.73 + 0.380 \cdot T; \\ &\text{steam:} \quad \mu = -9.82 + 0.3606 \cdot T. \end{aligned} \tag{35}$$

The viscosity of the gas is approximately equal to the weighted average of these viscosities, or

$$\mu = aT + b, \tag{36}$$

with

$$\begin{aligned} a &= 0.365 \cdot \lambda (1-\omega) + 0.38 (1-\lambda)(1-\omega) + 0.3606 \cdot \omega, \\ b &= 64.85 \cdot \lambda (1-\omega) + 36.73 (1-\lambda)(1-\omega) - 9.82 \cdot \omega. \end{aligned} \tag{37}$$

For simplicity, and as a very good approximation, it will be assumed that the pressure within the drying column is constant and denoted by p_0. Denoting the densities of the gas components, at 100°C and 101 kPa, by σ_i, and the partial pressures by p_i, the density of the gas in the drying column, σ, at temperature T, is then, finally, given by

$$\sigma = \frac{1}{101} \cdot \frac{373}{T + 273} \sum_{i=1}^{3} p_i \, \sigma_i. \tag{38}$$

Values for the densities σ_i are given in Table 5.

Let $\sum = \omega/18 + \lambda(1-\omega)/28 + (1-\lambda)(1-\omega)/44$; then the partial pressures are given by the expressions

$$\begin{aligned} &\text{nitrogen: } 0.0357 \cdot p_0 \cdot \lambda(1-\omega)/\textstyle\sum; \\ &\text{carbon dioxide: } 0.0238 \cdot p_0 (1-\lambda)(1-\omega)/\textstyle\sum; \\ &\text{steam: } 0.0556 \cdot p_0 \cdot \omega/\textstyle\sum. \end{aligned}$$

3.4. Equations of Motion. With the characteristics of the drying gas now determined, the drag force acting on a single particle of diameter s due to the relative velocity v_r is also determined and can be written in the form

$$F_d(l) = \left[0.157 + 10.2 \cdot \left(\frac{\mu}{s v_r \sigma} \right)^{0.8} \right] s^2 \sigma v_r^2, \tag{39}$$

where l is the vertical coordinate within the drying column, measured upwards from the point at which the crushed coal is injected into the drying column, and all the parameters on the right-hand side are dependent on l.

In addition to the drag force, there is the force of gravity, F_g, acting on the particle; it is given by

$$F_g(l) = 9.81 \cdot m, \quad \text{with } m = 0.5236\rho \cdot s^3, \tag{40}$$

where ρ is the density of the particle. The equation of motion of the particle is then

$$\frac{dv}{dt} = \frac{1}{m}\left(F_d - F_g\right), \tag{41}$$

where v is the upward velocity of the particle. However, the subsequent numerical calculations require v as a function of l rather than of t, or $dv/dl = dv/dt \cdot dt/dl$. So consider a particle with velocity $v(l)$ at position l and moving to $l + dl$ in the time dt, at which point its velocity is $v(l + dl) = v(l) + dl$; then

$$\frac{dv}{dl} = \frac{dv}{dt} \cdot \frac{1}{v}, \tag{42}$$

and the equation of motion is now

$$\frac{dv}{dl} = \frac{1}{m \cdot v}\left(F_d - F_g\right). \tag{43}$$

As it is usually assumed that the particles are injected horizontally into the drying column, the initial condition is $v(l = 0) = 0$, in which case (43) implies that $dv/dl = \infty$, which is clearly not useful, and the way around this apparent problem is discussed in Section 5.2. However, it is of interest to investigate the time and distance scales we are confronted with in this initial part of the drying process, and to that end we can define a *characteristic distance*, δ, as the distance a particle would travel until its velocity reaches the gas velocity if the acceleration remained constant as given at $t = 0$.

For convenience in this investigation we shall take the dependence of μ and σ on the temperature, T [°C], to be approximated by the two expressions $\sigma = 310/(T + 273)$ and $\mu = (150 + 0.355T) \cdot 10^{-7}$. That is, we are neglecting the influence of the changing gas composition, but this is not too bad of an approximation, as can be verified using values published in Appendix A of [3] and is also demonstrated by the actual calculations in the model (see Section 4.2). With these approximations, the expression for C_d, (34), becomes

$$C_d = 0.4 + \frac{f(T) \cdot 10^{-3}}{(sv)^{0.8}}, \tag{44}$$

where the relative velocity is now simply the hot gas velocity v and the function $f(T)$ is closely approximated by the expression

$$f(T) = 8.956 \cdot 10^{-6}T^2 + 0.01747 \cdot T + 3. \tag{45}$$

The acceleration at $t = 0$ is then given by the expression

$$\left[0.4 + \frac{f(T) \cdot 10^{-3}}{(sv)^{0.8}}\right] \frac{0.179 \cdot v^2}{(T + 273)\, s} - 9.81, \tag{46}$$

Table 6: The characteristic length at the injection point of the crushed coal, in meters, as function of the hot gas temperature, T, in °C, and the particle diameter, s, in mm, for a hot gas velocity of 25 m/s.

"$T \setminus s$"	0.1	0.2	0.5	1.0	2.0	5.0
500	0.10	0.32	1.30	3.60	10.33	80
600	0.10	0.32	1.33	3.79	11.33	116
700	0.10	0.31	1.34	3.94	12.22	177
800	0.10	0.31	1.35	4.05	13.00	303
900	0.09	0.30	1.35	4.13	13.66	718

and the characteristic distance is just v^2 divided by twice this acceleration. As an example, the characteristic length (m) as a function of gas temperature (°C) and particle diameter (mm) is shown in Table 6 for the case of a hot gas velocity of 25 m/s.

As the values in Table 6 demonstrate, for very small diameters (e.g., $s < 0.1$ mm) the acceleration at the injection point is so great that it is practically impossible to model the particle trajectories with any useful accuracy, and the simplest approach is to say that the particles attain their ultimate velocity (the gas velocity minus the entrainment velocity; see next section) in a linear manner within the first "slice" of the drying column (see Section 5.2 for a definition of "slice").

As the particle travels upward in the drying column, it dries by ejecting water in the form of steam, and the water content of the particle, initially equal to x, decreases to w. There are then two extreme possibilities: either the particle volume remains unchanged and the density decreases or the volume decreases in proportion to the ejected water and the density remains unchanged. The actual situation may be anywhere between these two extremes, and to account for this we introduce the *shrinkage parameter* ε, with $0 \le \varepsilon \le 1$, such that a value of 1 means that the particle shrinks by all the volume of ejected water and a value of 0 means that there is no shrinkage.

Consider a coal particle to consist of two components: water (initially a fraction x) and the rest (about half-and-half fixed carbon and volatile matter, with a small amount of ash and some air in the form of porosity). Initially, the particle has a diameter s_0, a volume $0.5236 \cdot {s_0}^3$, and a density ρ_0, and the mass of the rest is $0.5236\,(1 - x)\rho_0 {s_0}^3$. Assuming the absence of any devolatilisation the mass of this component remains constant as the water is evaporated, and let w be the fraction of the water remaining. Then, for the case $\varepsilon = 0$, the density is given by $\rho = \rho_0(1 - x(1 - w))$ and the diameter remains unchanged; for the case $\varepsilon = 1$, the diameter is given by $s = s_0(1 - x\rho_0(1 - w))^{1/3}$ and the density by $\rho = \rho_0(1 - x(1 - w))/(1 - x\rho_0'(1 - w))$. For the general case,

$$\rho = \rho_0 \frac{1 - x(1 - w)}{1 - \varepsilon \cdot x \cdot \rho_0'(1 - w)}, \qquad s = s_0\left(1 - \varepsilon \cdot x \cdot \rho_0'(1 - w)\right)^{1/3}, \tag{47}$$

where ρ_0' is the density relative to that of water (i.e., $\rho_0' = \rho_0/1000$). This shrinking is discussed further in Section 5.4.

Table 7: The entrainment velocity, v_0, in m/s, as a function of the particle diameter (columns, in mm) and the gas temperature (rows, in °C).

	0.1	0.2	0.5	1.0	2.0	5.0
100	0.33	0.88	2.76	5.33	8.85	15.27
200	0.30	0.82	2.73	5.57	9.60	16.98
300	0.28	0.77	2.67	5.70	10.20	18.45
400	0.26	0.73	2.60	5.77	10.67	19.74
500	0.25	0.70	2.53	5.79	11.04	20.89
600	0.24	0.67	2.46	5.78	11.32	21.91
700	0.23	0.64	2.39	5.74	11.54	22.83
800	0.22	0.62	2.32	5.68	11.71	23.65

3.5. Entrainment Velocity. The entrainment velocity, v_0, for a coal particle in the drying column is that gas velocity for which the particle does not move in the vertical direction, that is, the velocity at which the drag force equals the gravitational force, or

$$F_d(v_0) - 9.81m = 0, \tag{48}$$

where m is the mass of the particle, and the gravitational acceleration equals 9.81 m/s^2. Or, using (32) for F_d and if we, for the purpose of this subsection, assume an average density for the coal particles in the drying column of 1300 kg/m^3, then we obtain

$$v_0 = 130.4\sqrt{\frac{s}{\sigma C_d}}. \tag{49}$$

If we further, for the present purpose, set $\varepsilon = 0$ and use (44) for C_d, (49) becomes a nonlinear equation for v_0, of the form

$$v_0^2 + av_0^{1.2} - b = 0, \tag{50}$$

with

$$\begin{aligned} a &= 0.0025 \cdot s^{-0.8} \cdot f(T), \\ b &= 137 \cdot s(T + 273). \end{aligned} \tag{51}$$

A set of results is shown in Table 7.

For the purpose of the numerical model of the drying process (see Section 4.2), the results in Table 7 can be approximated by the following expression:

$$v_0 = as^2 + bs - 0.3, \tag{52}$$

with

$$\begin{aligned} a &= 0.000307 \cdot T - 0.537, \\ b &= 0.00086 \cdot T + 5.68. \end{aligned} \tag{53}$$

The drying column diameter can then be chosen so as to ensure that the drying gas velocity is a certain amount above the normalised entrainment velocity; the multiplication factor is the *entrainment assurance factor*, with a value typically in the range 1.25–1.5.

As discussed in the previous section, small particles (i.e., with $s < 0.1$ mm) are accelerated so rapidly at the injection point that the numerical integration of the equation of motion becomes impractical. Instead, we shall simply assume that they attain the entrainment velocity linearly in the first integration step (or "slice") and set the entrainment velocity equal to 0.2 m/s.

It is interesting to note some entrainment velocities reported in the literature. In Wypych [13] we find, for alumina pellets with a diameter of 0.1 mm in air at 20°C and 101 kPa, the two values 0.74 m/s and 0.79 m/s, whereas for crushed coal at 6 mm diameter the values are 15.65 m/s and 15.89 m/s.

3.6. The Significance of Particle Shape. As already discussed in Section 3.1, the fact that the crushed coal particles injected into the drying column are not spherical, while most of the theoretical and experimental information relates to spherical particles, has led to a somewhat peculiar situation. First of all, if the particles are characterised by the diameter of spherical particles of the same volume (or mass), the distribution (by mass) of these "equivalent" particles differs slightly from that obtained directly from the sieving results. Secondly, many of the results obtained for these "equivalent" spherical particles have to be corrected for the lack of sphericity. A review of the subject matter of particulate flows, as of the year 2000, can be found in [14, 15].

Starting with the dynamics, any shape departing from that of a sphere will have a drag coefficient greater than that of a sphere of the same volume, and while the body of experimentally determined values of the drag coefficient is not as extensive as for spherical particles, there is a reasonable understanding of the influence of particle shape, much of it based on the seminal experiments of Pettyjohn and Christiansen [16]. In particular, it is accepted that the influence of nonsphericity on the drag coefficient can be described by a single parameter, the previously introduced *sphericity*, ψ, and a function proposed by Ganser [17] and Haider and Levenspiel [18] has been shown by Hartman et al. [5] to give an excellent representation of the experimental data. Based on data presented in [14, 15], the influence of sphericity on the drag coefficient, as a function of the Reynolds number, can be determined and is shown in Figure 9.

3.7. Oxygen Level. As mentioned in Section 1.1, in those cases where the material to be dried is combustible and potentially explosive in pulverised form, a central issue in the control of the drying process is maintaining an inert atmosphere or, in other words, maintaining a low oxygen content in the drying gas. The oxygen content is determined by a number of the process parameters, but the general situation can be assessed in terms of the basic process diagram shown in Figure 10 (refer also to Figure 1).

Then, using the notation for the flows indicated in Figure 10 and using the notation introduced in Section 2.1,

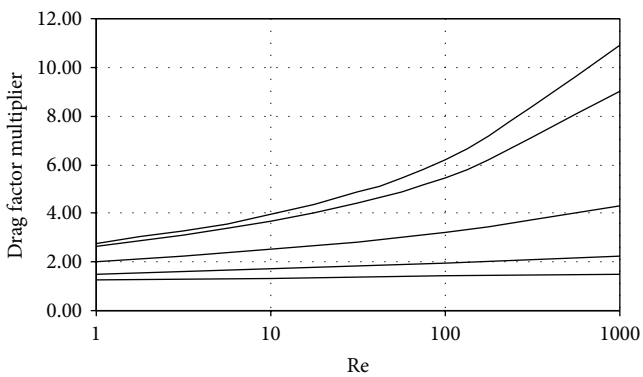

FIGURE 9: The ratio of drag coefficient for a nonspherical particle to that of a sphere, as a function of the Reynolds number (Re), for sphericity values of (from bottom to top) 0.95, 0.9, 0.8, 0.6, and 0.4, based on data given in [3].

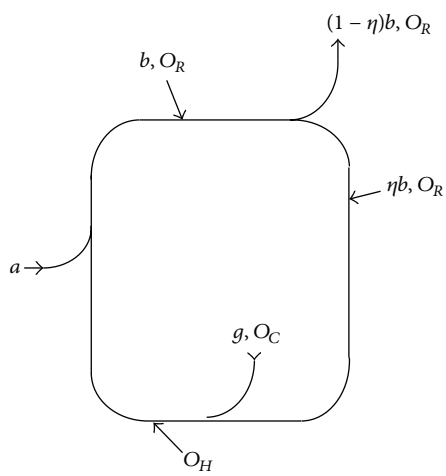

FIGURE 10: Gas circuit, with flows (by weight) and oxygen contents.

we obtain the following expressions relating to the various quantities:

$$O_H = \frac{g \cdot O_C + \eta \cdot b \cdot O_R}{g + \eta \cdot b},$$
$$b = \left(g + \frac{x-y}{1-x}\right)\frac{1}{1-\eta}, \tag{54}$$

$$O_R = \frac{g \cdot O_C}{g + (x-y)/(1-x)}. \tag{55}$$

The oxygen content of the combustion gas, O_C, will depend on the fuel used to generate the gas, as expressed by the quantity of air needed for stoichiometric combustion, but to a first approximation it can be taken to be the following function of the excess air, κ:

$$O_C = 0.23\frac{\kappa}{1.1+\kappa}, \tag{56}$$

which, with assumption (ii) in Section 2.1, gives $O_C \approx 3.5\%$. The value of g is determined by the fuel and given by (17),

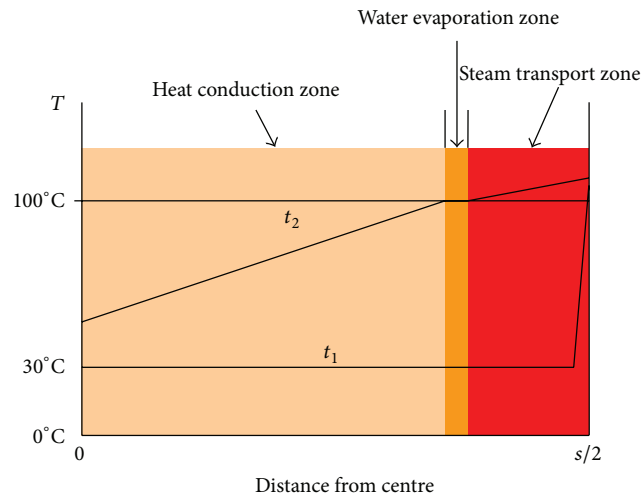

FIGURE 11: Simplified representation of the thermal processes taking place in a single particle of diameter s at some time t_2 after injection into the drying column, with the temperature shown as a function of distance from the centre of the particle. The temperature curve labelled t_1 indicates the situation just after the particle is injected into the drying column.

and so, for any given case, the oxygen level, O_H, can be determined for the range of operating points and provide assurance that it will remain below the explosion limit.

4. Heat Transfer

4.1. Heat Transfer between the Gas and a Single Particle. A particular feature of the present model is that it takes explicit account of the fact that the majority of the moisture is contained within the particles. This is in contradistinction to most commercial designs, which assume that the moisture is mainly surface moisture [19].

Consider a single coal particle, taken for the following development to be spherical, with diameter s. It is initially at ambient temperature, say 30°C, but on introduction into the drying column, its surface temperature will go immediately to just over 100°C, and water on or near the surface starts to evaporate, as shown in Figure 11. As time progresses, the evaporation moves inward, and the volume between the evaporation and the surface serves to transport the steam, which becomes gradually more superheated, to the surface. From the evaporation zone heat is also conducted inward, heating the coal there and the water contained in it.

The picture presented in Figure 11 contains the major assumption that as long as there is water left in the particle to evaporate, the surface temperature will not rise appreciably above 100°C. That is, the effective thermal resistance of what is labelled as the steam transport zone in Figure 11 is much less than the thermal resistance equivalent to the heat transfer between the gas and the surface of the particle.

The energy (heat) transferred from the gas to a single particle of diameter s per second is reasonably well represented

by the following expression [3]:

$$Nu = 2 + \left(0.4 \cdot \mathrm{Re}^{1/2} + 0.06 \cdot \mathrm{Re}^{2/3}\right) \mathrm{Pr}^{0.4} \left(\frac{\mu}{\mu_s}\right)^{1/4}, \quad (57)$$

where

$$Nu = \frac{h' \cdot s}{k}; \qquad \mathrm{Pr} = \frac{\nu}{\alpha}; \quad (58)$$

and h' = heat transfer coefficient (W/m$^{2\circ}$C), k = thermal conductivity of gas (W/m °C), α = thermal diffusivity, k/σc$_p$ (m^2/s), μ = viscosity (Ns/m^2), μ_s = viscosity at the temperature of the particle surface (110°C), and ν = kinematic viscosity, μ/σ (N·s·m/kg).

The value of Pr can be taken as constant and equal to 0.7 (see, e.g., Table 2 of [20]). An expression for μ was given in (37), and the thermal conductivity, k, as given, for example, in the Table cited above, can be approximated by the expression $(27.1 + 0.052 \cdot T) \cdot 10^{-3}$. The Reynolds number, Re, was introduced in (33).

With this, the energy transferred per second to a particle with diameter s and located at a position in the drying column where the gas is characterised by λ, ω, and T and where the relative velocity is v_r can be written as

$$h(s; \lambda, \omega, T, v_r) = (85.1 + 0.163 \cdot T)(T - 110) \cdot s \cdot 10^{-3} \times \left[2 + 0.867\left(0.4 \cdot \mathrm{Re}^{1/2} + 0.06 \cdot \mathrm{Re}^{2/3}\right) \times \left(\frac{\mu}{\mu_s}\right)^{1/4}\right]. \quad (59)$$

We can now check if the assumption implicit in Figure 11 is justified. By evaluating (59), we find the energy transferred per second, $h(s)$ (W), to a particle of diameter d at a gas temperature of 618°C (an arbitrary, but typical, gas temperature at the beginning of the drying process) is as shown in the second column of Table 8. The third column displays the equivalent thermal resistance, $R_s = (T - 110)/h(s)$ (°C/W). Let δ be the thickness of a surface layer of the particle, expressed as a fraction of s; then the thermal resistance of this layer, R_c, is given by

$$R_c(\delta) = \frac{1}{0.33 \cdot 4\pi} \int_{(s/2)(1-2\delta)}^{s/2} \frac{dx}{x^2}, \quad (60)$$

where we have taken the thermal conductivity of the subbituminous coal to be 0.33 W/m°C [21]. If this is evaluated for $\delta = 0.103$, which corresponds to the layer having a volume equal to half that of the particle (and which can be taken as an average distance; the heat has to penetrate in order to evaporate water), the results are displayed in the fourth column.

The data presented in Table 8 shows that our assumption, $R_s/R_c \gg 1$, is not justified, except for very small particles.

Table 8: Heat transferred per second to a particle of diameter s, $h(s)$, in a gas of temperature 618°C, and the corresponding surface thermal resistance, R_s, and internal coal resistance, R_c, as well as the ratio R_s/R_c.

s (mm)	$h(s)$ (W)	R_s (°C/W)	R_c (°C/W)	R_s/R_c
3	4.5913	85	83	1.02
1.5	1.6102	241	167	1.45
0.75	0.5534	703	333	2.11
0.375	0.1982	1962	667	2.94
0.1875	0.0734	5295	1333	3.97
0.09375	0.0274	14211	2667	5.33
0.046875	0.0107	36313	5333	6.81
0.023438	0.0046	84018	10666	7.88

It appears that the surface temperature is not always slightly above 100°C, but somewhere between 100°C and 100 + (618 − 100) $R_c/(R_s+R_c)$ °C and that we may not be able to neglect the superheating of the steam inside the particle. To investigate the latter issue, let the heat flow that reaches the evaporation zone be denoted by h_e (J/s); then the amount of steam generated per second in the particle equals $h_e/2255000$ (kg/s). The energy per second used to superheat this steam to the surface temperature, T_s, is $2h_e(T_s - 100)/2255$ (J/s), where the specific heat capacity of steam has been taken to be equal to 2 kJ/kg °C. Consequently, the influence of the superheating on the drying of a particle is a reduction by a factor given approximately by the expression

$$\frac{h_e}{h} = \frac{h_e}{h_e + h_s} = \frac{1}{1 + (T_s - 100)/1125}. \quad (61)$$

This reduction is not negligible, but our approach is now to at first neglect it in the determination of h and then apply it as a correction factor once a value of h has been found by the following successive approximation method.

Consider a particle of diameter s. Assuming that the moisture is distributed uniformly throughout its volume, then, if the remaining fraction of the moisture is w, the distance of the evaporation zone from the surface is equal to $s(1-w^{1/3})/2$. Using (60), the corresponding effective thermal resistance, R_c, is then given by

$$R_c = \frac{0.965}{s} \cdot \frac{1 - w^{1/3}}{w^{1/3}}. \quad (62)$$

The surface temperature, T_s, is just $100 + h \cdot R_c$ and inserting this into (59), we can, in principle, solve for the corrected value of h. However, in that equation, T_s not only is substituted for our assumed value of 110°C but also enters into the expression for μ_s, so that we cannot get an explicit expression for h. Instead, we assume a value, h^*, calculate h, and then reduce the difference between h and h^* by successive approximation. Once the value of h has been determined, the correction factor in (61) is applied before calculating the amount of water evaporated.

The steam leaving the particle is now already superheated to the surface temperature, T_s, and so needs only to be further

superheated to the gas temperature. This is calculated using (22), but with $T - T_s$ substituted for $T_x - 140$.

4.2. Macroscopic Heat Transfer. Turning now from a single particle to the two-component fluid (gas/coal) in the drying column, consider a column with internal cross-section A and length L (measured from the coal injection point). At any level l in the column, let the density of coal consisting of particles with s in the range s to $s + ds$ be denoted by $\xi(s, l)ds$ (measured in kg/m^3); then

$$\xi(l) = \int_0^{s_0} \xi(s, l)\, ds \tag{63}$$

is the total density of coal particles at the level l. Also, as the particles move with a velocity $v(s, l)$, the total flow of coal through a cross-section of the column at level l is given by the expression

$$M(l) = A \int_0^{s_0} \xi(s, l) \cdot v(s, l)\, ds, \tag{64}$$

and at the injection point, $l = 0$, this must equal the rate of crushed coal injection, to be denoted by M_0, and

$$\xi(s, l = 0)\, ds = M_0 \frac{q(s)\, ds}{A \cdot v(s)}. \tag{65}$$

However, as the vertical particle velocity at that point is zero, it would seem to imply that the density is infinite. To overcome this situation, which arises only as a result of our idealised treatment of the injection process, our numerical calculation will consider "slices" of the drying column with thickness dl and use the average velocity within that slice (see Section 5.3).

The mass of a particle with diameter s is $0.5236\rho \cdot s^3$ so the density (in particles per m^3) of particles with s in the range $s + ds$ is $\xi(s, l)ds$ divided by this quantity. Then, for a "slice" of the drying column of thickness dl, the energy transferred between gas and the coal particles with diameters in the range s to $s + ds$ per second, $H(s, l)dl \cdot ds$, is given by

$$\begin{aligned} H(s, l)\, dlds = {} & 1.91 \cdot h(s; \lambda, \omega, T, v_r)\, \xi(s, l) \\ & \cdot \rho^{-1}(s, l) \cdot s^{-3} \cdot A \cdot dl \cdot ds. \end{aligned} \tag{66}$$

In (66), v_r is determined by using (14) and $\rho(s, l)$ is determined by (15). Of course, both quantities depend on the drying gas velocity $v_0(l)$, which itself depends on $H(l)$, so because of this coupling, as well as the highly nonlinear nature of the expressions for the various quantities involved in (32), there is no analytic expression for $H(l)$. Therefore, in order to convert the model of the flash drying process developed in the foregoing into a practical tool for plant design, one needs to create a corresponding computer application. That is, in itself, not a major or difficult task, but the next section raises a number of issues that need to be taken into consideration when developing the program.

Table 9

The index (I) means	
The value in the middle of the I-th slice for	The value at the end of the I-th slice for
Acceleration	Temperature
	Velocity

5. Numerical Evaluation Issues

5.1. The Independent Variables. The basic function of any numerical representation of the model is to carry out the numerical integration of (66), which, in effect, means the coupled integration of the dependent variables involved in that equation, such as temperatures, velocities, and gas compositions. These dependent variables are functions of the two independent variables l, position along the drying column, measured from the injection point, and s, the particle diameter. These two continuous variables are represented as discrete variables by two indices: (I) for position along the column and (J) for the particle diameter. The position integration steps take into account that gas temperature and particle velocities vary much more rapidly at the bottom of the column than towards the top; the "slices" of the column have centre values, $X(I)$, and step sizes, DL(I) (both as fractions of the column length, L), and for a choice of 24 "slices" a suitable division is shown in Table 10.

Note that when a variable, say $a(I)$, is a function of position along the column, it can mean either its value in the middle of the Ith slice or at the end of the slice as shown in Table 9.

The particle diameter, s, is represented by discrete classes, corresponding to the sieving results. An example of an application with eight classes (i.e., $J = 1$ to 8, with 1 corresponding to the largest particles and 8 to the smallest, as used already in Table 8) is shown in Table 11; if the sieving results are initially available in some other form, they must either be converted to the chosen number of classes or the application must be designed to handle a variable number of classes.

5.2. Integration Algorithm. In developing a program, an important observation is that, of the many parameters that vary with position within the drying column, only two are rapidly varying: the gas temperature, $T(I)$, and the particle velocities, $v(J, I)$. Consequently, the changes in these two variables, from the start of a "slice" to the end of the "slice," are determined using what is in effect an improved Euler integration algorithm, first based on the values of all the other parameters at the beginning of the "slice", then at the end of the "slice", and then using the average to compute the values of these two variables at the end of the "slice". The values of all the other parameters are determined at the end of this algorithm. A step in the integration therefore takes the form shown in Figure 12.

The differential equation for the velocity function is given by (41); however, for the numerical integration we need to

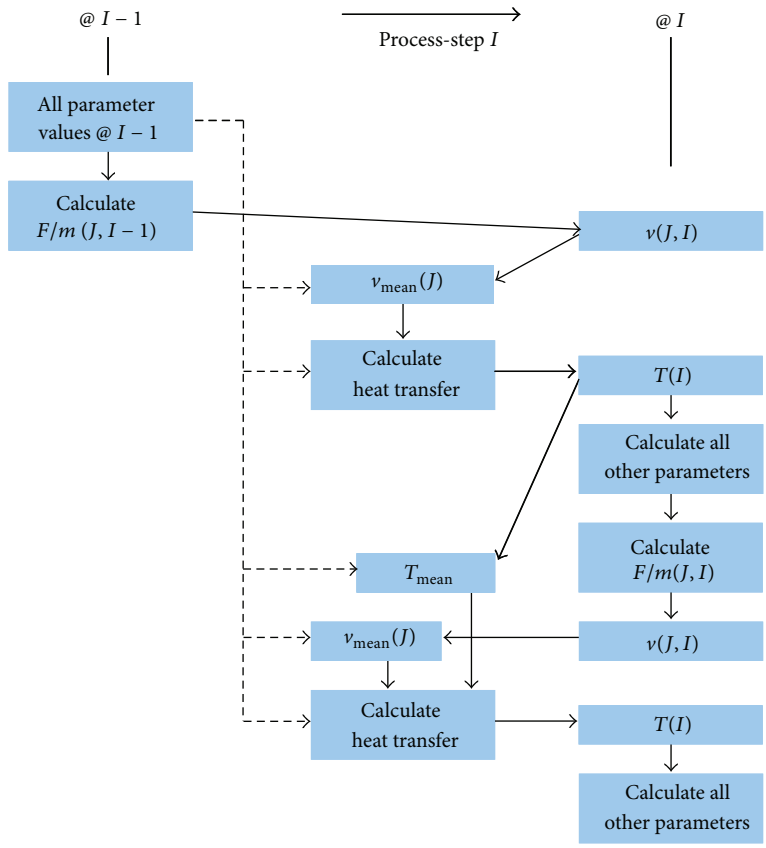

Figure 12: Calculation process for a single step in the numerical integration of (66).

proceed as follows. Consider the movement of a particle from l to $l+dl$ in the time dt, with the velocity changing from $v(l)$ to $v(l+dl)$ by dv under the acceleration F/m. Then $dv = dt \cdot F/m$ and

$$dl = \left(v(l) + \frac{dv}{2}\right) dv \cdot \frac{m}{F},$$
$$(dv)^2 \cdot \frac{m}{2} + m \cdot v dv - F dl = 0. \tag{67}$$

The solution to this equation is

$$v(l + dl) = \left(v^2(l) + 2dl \cdot \frac{F}{m}\right)^{1/2}. \tag{68}$$

5.3. Initial Values. In order to start the recursive integration process, it is necessary to generate the starting values, that is, for $I = 1$. As was mentioned following (43), it is generally true that $v(I = 0) = 0$, which is not an admissible value as far as the integration algorithm is concerned, so a different approach is required for the first step. It consists of first calculating the gas density at $x = 0$ and then the resultant gas velocity (as the mass flow is known from the input data). The particle accelerations at $x = 0$ then follow from (46), and this value is used to determine the particle velocities and densities at $x = x(1)$. The heat transfer in the short distance from $x = 0$ to $x(1)$ is calculated using the mean of these particle velocities and densities.

5.4. Unequal Drying. Particles with smaller diameters will dry faster than the larger ones, and below some diameter the particles will be completely dry prior to reaching the end of the drying column. This is taken into account by first calculating the initial (i.e., at injection) amount of water contained in each particle class and then keeping track of the cumulative amount of water evaporated from each class. At the point where the cumulated amount reaches the initial amount, the heat required to elevate the coal temperature from its surface temperature to the gas temperature is subtracted from the gas, and from then on the coal in that class gives up heat as it progresses upward in the drying column in equilibrium with the gas. Heating the coal in a class within a single "slice" is, of course, an approximation that leads to a local distortion in the temperature profile, but the error in the overall drying process is small.

5.5. Particle Shrinkage. The simple picture of coal particles progressing upward with only their water content and temperature changing is complicated by the fact that as water is evaporated the coal particles shrink and so a fraction of the particles in a class move into the next lower class (i.e., higher value of J).

Consider the "slice" of the column labelled by I and denote the mass throughput of coal in the size class J in the bottom of the "slice" by $M(J, I - 1)$ (refer to (64)) and the amount of water evaporated from the size class J in that

Table 10: The subdivision of the length of the drying column into 24 discrete "slices" for the purpose of performing a numerical integration of (66).

I	X	Step
1	0.001	0.000–0.002
2	0.003	0.002–0.004
3	0.010	0.004–0.016
4	0.022	0.016–0.028
5	0.034	0.028–0.040
6	0.050	0.04–0.06
7	0.070	0.06–0.08
8	0.090	0.08–0.10
9	0.110	0.10–0.12
10	0.130	0.12–0.14
11	0.150	0.14–0.16
12	0.170	0.16–0.18
13	0.190	0.18–0.20
14	0.225	0.20–0.25
15	0.275	0.25–0.30
16	0.325	0.30–0.35
17	0.375	0.35–0.40
18	0.425	0.40–0.45
19	0.475	0.45–0.50
20	0.550	0.50–0.60
21	0.650	0.60–0.70
22	0.750	0.70–0.80
23	0.850	0.80–0.90
24	0.950	0.90–1.00

Table 11: For the purpose of the numerical calculations, the particle size, s, is divided into discrete classes. These have been chosen so as to correspond to the number and mesh sizes of sieves commonly used to determine the particle size distribution of the crushed coal.

J	s	Δs
1	3	2–5
2	1.5	1-2
3	0.75	0.5–1
4	0.375	0.25–0.5
5	0.1875	0.125–0.25
6	0.09375	0.0625–0.125
7	0.046875	0.03125–0.0625
8	0.023438	0.01–0.03125

"slice" by $\mathrm{DW}(J,I)$. As a result of the evaporation, the mass of the coal is reduced by $\mathrm{DW}(J,I)$; that is, $M(J,I) = M(J,I-1) - \mathrm{DW}(J,I)$, and the volume of the coal particles will also be reduced. However, experience shows that the reduction is somewhat less than the volume of evaporated water; as indicated by the *shrinkage factor* ε introduced in Section 3.4, the volume of coal is reduced by $\varepsilon \cdot \mathrm{DW}/1000$, where the density of water is 1000 kg/m^3 and the particle density at the top of the "slice," $\rho(J,I)$, is given by the following expression:

$$\rho(J,I) = \frac{M(J,I-1) - \mathrm{DW}(J,I)}{M(J,I-1)/\rho(J,I-1) - \varepsilon \cdot \mathrm{DW}(J,I)/1000}. \tag{69}$$

The shrinkage in volume means a reduction in the particle diameters, denoted by shift (J,I) and it is given by the expression

$$\mathrm{Shift}(J,I) = s(J)\left[1 - \left[1 - \varepsilon\frac{\rho(J,I-1)\cdot \mathrm{DW}(J)}{1000\cdot M(J,I-1)}\right]^{1/3}\right]. \tag{70}$$

The result of this process is therefore twofold. Firstly, the particles lose some of their mass, so that the particle mass transport rate, $M(J,I)$, as introduced in (64), is reduced by $\mathrm{DW}(J,I)$. Secondly, the effect of the shift in the boundaries is that a corresponding fraction of the mass in size class J is moved into class $J+1$, so that there is a gradual change in the particle size distribution toward smaller diameters as the coal moves upward in the column, as expressed by the algorithm

$$\begin{aligned} q(J,I) = {} & q(J,I-1)\left[1 - \frac{\mathrm{Shift}(J,I)}{\Delta s(J)}\right] \\ & + q(J-1,I-1)\left[\frac{\mathrm{Shift}(J-1,I)}{\Delta s(J)}\right]. \end{aligned} \tag{71}$$

The overall effect is to change the coal density according to the following, generalised version of (63):

$$\xi(J,I) = \frac{2\cdot M(J,I-1)\cdot q(J,I-1)}{A\cdot(v(J,I-1)+v(J,I))}. \tag{72}$$

6. Conclusion

The model of the flash drying process presented in this paper was initially developed for the specific purpose of drying subbituminous coal and was successfully used for that purpose in the case of a 60 MW plant, although the results of that application remain restricted by confidentiality agreements. However, the present version is of sufficient generality to be easily applied to the flash drying of other substances.

The model, when represented in the form of a computer program, is a valuable tool for the basic design of flash drying plant, in that, for given material and throughput parameter values, it allows trade-offs between plant parameters, such as drying column length and cross-section, gas temperature, and recycle ratio. It also permits investigations regarding the sensitivity of a given design to variations in the input material parameters and the development of suitable control strategies. It is also very useful in performing a design trade-off between the cost of high-temperature materials and the cost of handling increased gas flows, as indicated by Figure 2.

Conflict of Interests

The author declares that there is no conflict of interests regarding the publication of this paper.

Acknowledgments

It is a pleasure to acknowledge the support of this work, through reviews and comments, by the following persons: W. G. Kalb (of TraDet Inc.), K. Clark (of White Energy), and C. Needham and B. Smeaton (both of SKM). The valuable comments of the anonymous reviewer are also acknowledged.

References

[1] S. M. El-Behery, W. A. El-Askary, K. A. Ibrahim, and M. H. Hamed, "Porous particles drying in a vertical upward pneumatic conveying dryer," *World Academy of Science, Engineering and Technology*, vol. 53, pp. 1337–1351, 2009.

[2] Y. Li -H and J. L. Skinner, "Development and validation of a process simulator for drying subbituminous coal," *Chemical Engineering Communications*, vol. 49, pp. 99–118, 1988.

[3] F. P. Incopera and D. P. DeWitt, *Fundamentals of Heat Transfer*, John Wiley & Sons, 3rd edition, 1990.

[4] R. C. Weast, *Handbook of Chemistry and Physics*, CRC Press, 54th edition, 1973.

[5] M. Hartman, O. Trnka, K. Svoboda, and V. Vesely, "Influence of particle shape on the drag coefficient of isometric particles," *Collection of Czechoslovak Chemical Communications*, vol. 59, pp. 2583–2594, 1994.

[6] S. Laín and M. Sommerfeld, "A study of the pneumatic conveying of non-spherical particles in a turbulent horizontal channel flow," *Brazilian Journal of Chemical Engineering*, vol. 24, no. 4, pp. 535–546, 2007.

[7] S. Martin and L. Santiago, "Transport characteristics of isometric non-spherical particles in turbulent flow," *El Hombre y la Maquina*, no. 30, 2008.

[8] E. Kaya, R. Hogg, and S. R. Kumar, "Particle shape modification in comminution," *KONA*, vol. 20, pp. 188–195, 2002, http://www.kona.or.jp/search/20_188.pdf.

[9] J. P. Matthews, S. Eser, P. G. Hatcher, and A. W. Scaroni, "The shape of pulverized bituminous vitrinite coal particles," *Hosokawa Powder Technology Foundation, KONA*, vol. 25, pp. 145–152, 2007.

[10] J. H. Perry, Ed., *Chemical Engineers' Handbook*, McGraw-Hill, 6th edition, 1984.

[11] M. L. de Souza-Santos, *Solid Fuels Combustion and Gasification: Modeling, Simulation, and Equipment*, Marcel Dekker, 2004.

[12] S. Keys and A. J. Chambers, *Scaling Pneumatic Conveying Characteristics for Pipeline Pressure*, The Centre for Bulk Solids and Particulate Technologies, University of Newcastle, 1996.

[13] P. Wypych, *Prediction & Scale-Up of "Steady-State" Operating Conditions, Lectures on Pneumatic Conveying*, University of Wollongong.

[14] M. Sommerfeld, *Theoretical and Experimental Modelling of Particulate Flows, A Lecture Series*, Von Karman Institute for Fluid Dynamics, 2000.

[15] R. D. Marcus, A. R. Reed, and A. J. Chambers, *Pneumatic Conveying of Bulk Solids, Course Notes*, TUNRA Bulk Solids Handling Research Associates, Department of Mechanical Engineering, University of Newcastle, Newcastle, Australia, 1986.

[16] E. S. Pettyjohn and E. B. Christiansen, "Effect of particle shape on free-settling rates of isometric particles," *Chemical Engineering Progress*, vol. 44, no. 2, pp. 157–172, 1948.

[17] G. H. Ganser, "A rational approach to drag prediction of spherical and nonspherical particles," *Powder Technology*, vol. 77, no. 2, pp. 143–152, 1993.

[18] A. Haider and O. Levenspiel, "Drag coefficient and terminal velocity of spherical and nonspherical particles," *Powder Technology*, vol. 58, no. 1, pp. 63–70, 1989.

[19] "GEA Process Engineering Inc," http://www.niroinc.com/food_chemical/flash_drying_concepts.asp.

[20] J. H. Keenan and J. Kaye, *Gas Tables*, John Wiley & Sons, 1946.

[21] J. M. Herrin and D. Deming, "Thermal conductivity of U.S. coals," *Journal of Geophysical Research B*, vol. 101, no. B11, pp. 25381–25386, 1996.